

SUPPORTING INFORMATION

Self-Templated Conversion of A Self-healing Metallogel into Active Carbon Quasiaerogel: Boosting Photocatalytic CO₂ Reduction by Water

Noohul Alam^a, Niwesh Ojha^b, Sushant Kumar^b and Debajit Sarma^{a*}

^aSolid State and Inorganic Chemistry Group, Department of Chemistry, Indian Institute of Technology Patna, Bihar 801106, India

^bGas-Solid Interaction Laboratory, Department of Chemical and Biochemical Engineering, Indian Institute of Technology Patna, Bihar 801106, India

*Corresponding Author, e-mail: debajit@iitp.ac.in

Number of Pages: 24

Number of Tables: 3

Number of Figures: 18

Table of Contents

Figure S1. The storage modulus and loss modulus measurement of Nd-SHMG-metallogel with (a) shear stress, and (b) angular frequency.	7
Figure S2. Dynamic shear stress sweep vs. gain modulus (G') and loss modulus (G'') of Nd-SSMG metallogel.....	8
Figure S3. Pore size distribution of Nd@NCA, Nd@NCA-1 and MF@NCA catalysts.	9
Figure S4. FTIR spectra of Nd@NCA and MF@NCA catalysts.....	10
Figure S5. CO ₂ -TPD analysis of Nd@NCA and MF@NCA catalysts.	11
Figure S6. Zeta potential plot of Nd@NCA and MF@NCA catalysts.....	12
Figure S7. (a-e) Elemental mapping of Nd@NCA catalyst.	12
Figure S8. (a-d) Elemental mapping of MF@NCA catalyst.....	12
Figure S9. EDX images of Nd@NCA and Nd@NCA-1 and MF@NCA catalysts.....	13
Figure S10. (a) The powder X-ray diffraction pattern of Nd@NCA, MF@NCA catalysts, and Carbon (ICSD database reference: 76767), (b) Raman analysis of Nd@NCA, and MF@NCA catalysts.....	14
Figure S11. XPS survey of (a) Nd@NCA, the deconvoluted peaks of (b) N 1s, and (c) C 1s for Nd@NCA. XPS survey of (d) MF@NCA, the deconvoluted peaks of (e) N 1s, and (f) C 1s for MF@NCA.....	15
Figure S12. (a) CO ₂ adsorption capacity of Nd@NCA, Nd@NCA-1 and MF@NCA catalysts. (b) Schematic illustration for the preparation of porous Nd@NCA-1, and MF@NCA materials through selective removal of metal from the pristine Nd@NCA catalyst.	16
Figure S13. UV-vis absorption spectra of (a) Nd@NCA, (b) Nd@NCA-1, and (c) MF@NCA catalysts, and Tuac's plots of (d) Nd@NCA, (e) Nd@NCA-1, and (f) MF@NCA catalysts. ...	17
Figure S14. Photoluminescence spectra of Nd@NCA, Nd@NCA-1 and MF@NCA catalysts.	18
Figure S15. The gas chromatograph for 200 ppm CH ₄ present in the standard gas mixture (composition: O ₂ , H ₂ , CO and CH ₄ : 200 ppm each and the rest is argon), (b) Gas chromatograph for various set of controlled/blank measurement.....	19
Figure S16. The CO ₂ reduced products obtained for Nd@NCA catalyst over three photocatalytic cycles.....	20
Figure S17. The carbon monoxide selectivity plot of CO over CH ₄	21
Figure S18. Time-dependent in situ DRIFT analysis for Nd@NCA catalyst using moist CO ₂ ..	22

Table S1. Surface area, pore size and pore volume of the as-synthesized catalysts.....23

Table S2. PL lifetime fitting parameters of **Nd@NCA**, **Nd@NCA-1** and **MF@NCA**. 23

Table S3. Comparison table of light driven photocatalytic CO₂ reduction with some of the reported benchmark catalysts. 24

Photoelectrochemical measurements. To perform the photoelectrochemical study, the working electrodes were fabricated by making a thin film of the as-synthesized **Nd@NCA** and **MF@NCA** catalysts on FTO glass substrate (1*2 cm²). Briefly, 20 mg of as-synthesized catalyst was mixed with 20 μ L Nafion solution and 2 mL of absolute ethanol to form a slurry, then coated on the precleaned FTO glass using the doctor-blade method and kept for drying at 70 °C for an hour. Afterwards, a 100 mL quartz cell containing 0.1 M Na₂SO₄ (pH = 7, 80 mL) with a Teflon top was utilised to assemble the three-electrode setup. The coated FTO glass acts as a working electrode, Pt wire as a counter electrode and Ag/AgCl as the reference electrode. The electrochemical impedance spectroscopy (EIS) was performed between 1 Hz to 80 kHz. Further, Mott-Schottky (MS) analysis was executed in the range of -1 to 0 V to find out the flat-band potential at 500 Hz, 1kHz and 1.5 kHz. 300 W Xe lamp (Sciencetech, Canada) was utilized to record the photo-transient response under the constant bias of 0.2 V.

Gas-phase CO₂ reduction. The ability of any catalyst to effectively alleviate the atmospheric carbon dioxide concentration through photo catalytically reductions of CO₂ using water and light is clean and sustainable technology. Therefore, the applicability of the as-synthesized **Nd@NCA** and **MF@NCA** catalysts were checked through the gas-phase photoreduction of CO₂ in the presence of photocatalyst, moisture and light. We have performed the reaction in absence of any sacrificial agent. Typically, we dispersed 50 mg of catalyst in 10 mL of Milli-Q water and sonicated for 30 minutes, then the mixture solution was directly poured onto the concave surface of two-necked quartz glass, and placed at 80 °C for overnight in the oven. After drying, a uniform thin film of catalyst was formed on the reactor's concave wall. The reactor's two apertures were then sealed with silicone rubber septa to create a closed system. Then, ultrapure carbon dioxide gas was passed continuously to avoid contamination with oxygen and valves were opened/closed multiple times to vent off any unwanted gas. Simultaneously, a gas chromatograph (GC) (Centurion Scientific, Model-5800) was used to check the gas composition inside the quartz reactor regularly by injecting a 1 mL gas-tight Hamilton syringe. When the reactor become free of oxygen, ultra-pure carbon dioxide gas was circulated through a Milli-Q water bubbler for 30 minutes at room temperature. The gas flow rate was set to 5 mL/min through a mass flow controller (Aalborg Instruments, USA). Additionally, 15 μ L of Milli-Q water was added to the reactor after that reactor was heated to 80 °C for 15 minutes. Subsequently, the reactor was then brought to

room temperature. We kept the reactor in the dark for two hours to achieve the carbon dioxide gas adsorption-desorption equilibrium with the catalyst. Next, Xe-lamp was turned on, and the temperature was maintained constant in the reaction system. After that, the obtained products were examined using gas chromatography equipped with a thermal conductivity detector (TCD), a flame ionised detector (FID), and a methanizer. Argon was used as the carrier gas, and the column material was molecular sieve (length 5 m, ID 2.1 mm).

In situ DRIFTS study. The DRIFTS study was conducted to identify reaction intermediates and elucidate plausible reaction mechanism for photocatalytic reduction of CO₂ with water under irradiation. The analysis was conducted using a thermo scientific Nicolet iS50 infrared spectrometers which was composed of the HARRICK praying Mantis reaction chamber and an MCT-A (Mercury Cadmium Telluride) detector, which was cooled by liquid nitrogen. About 5 mg of catalysts were loaded into the chamber after being mixed with KBr (1:100 w/w). Adsorbed species on the chamber and catalysts' surfaces were removed by heating them to 150 °C in a vacuum for two hours. Then, the chamber was naturally cooled down. Then, ultrapure carbon dioxide gas at a rate of 5 ml/min passed via a water bubbler in the Harrick cell for 30 minutes. Further, to achieve equilibrium between gaseous species and photocatalyst, batch system was formed by closing all inlet and outlet valves for 2 hours. After that, the background spectrum was obtained. Now, light from a 500W Xenon arc lamp was utilized to shine light through the quartz window. Subsequently, the data were acquired for 2 hours at a regular interval

In-situ DRIFTS study was also performed in the presence of isotopic-labelled ¹³CO₂. Specifically, a small amount (few ml) of ¹³CO₂ gas (Sigma Aldrich, 99 atom % ¹³C, <3 atom % ¹⁸O) was passed to the praying Mantis chamber directly from the gas canister. Prior to that, 50 μL of water droplets were added to the catalyst KBr mixture. Vacuum heating was performed at 150 °C for 30 minutes to eliminate surface impurities (if any). The mixture was then cooled naturally and kept in the dark for two hours to achieve adsorption-desorption equilibrium. After that, a 500 W Xe arc lamp was turned on and light was irradiated through the quartz window of the Harrick cell. Simultaneously, the FTIR spectrum in different time intervals was recorded.

Optical and electrical properties. The E_{fb} versus NHE can be calculated from the E_{fb} versus Ag/AgCl with help of the following equation.

$$E_{fb} \text{ versus NHE} = E_{fb} \text{ versus Ag/AgCl} + 0.197 \quad (\text{S1})$$

The E_{fb} versus NHE values of **Nd@NCA**, **Nd@NCA-1** and **MF@NCA** were calculated to be -0.623, -0.553 and -0.413 eV, respectively, by using equation S1. As we know, for n-type semiconductors the conduction band of the material is 0.1 eV lower value than E_{fb} , therefore, the conduction band (CB) of **Nd@NCA** and **MF@NCA** were found to be -0.723, -0.653 and -0.513 eV, respectively. Therefore, the corresponding valence band and conduction band can be calculated from the following equation.

$$E_{VB} = E_{CB} + E_g \quad (\text{S2})$$

Where E_{VB} represent the valence band edge potential, E_{CB} stands for conduction band edge potential, and E_g is the band gap of the materials. The VB of the **Nd@NCA**, **Nd@NCA-1** and **MF@NCA** of the catalysts were calculated to be 2.05, 2.297 and 3.22 eV, respectively. Based on the obtained data, the electronic band structure versus NHE is presented in figure 5g. The band alignment presented in figure 5g illustrated that all three **Nd@NCA**, **Nd@NCA-1** and **MF@NCA** photocatalysts possess desirable band edge positions to execute CO₂ gas reduction in the presence of light.

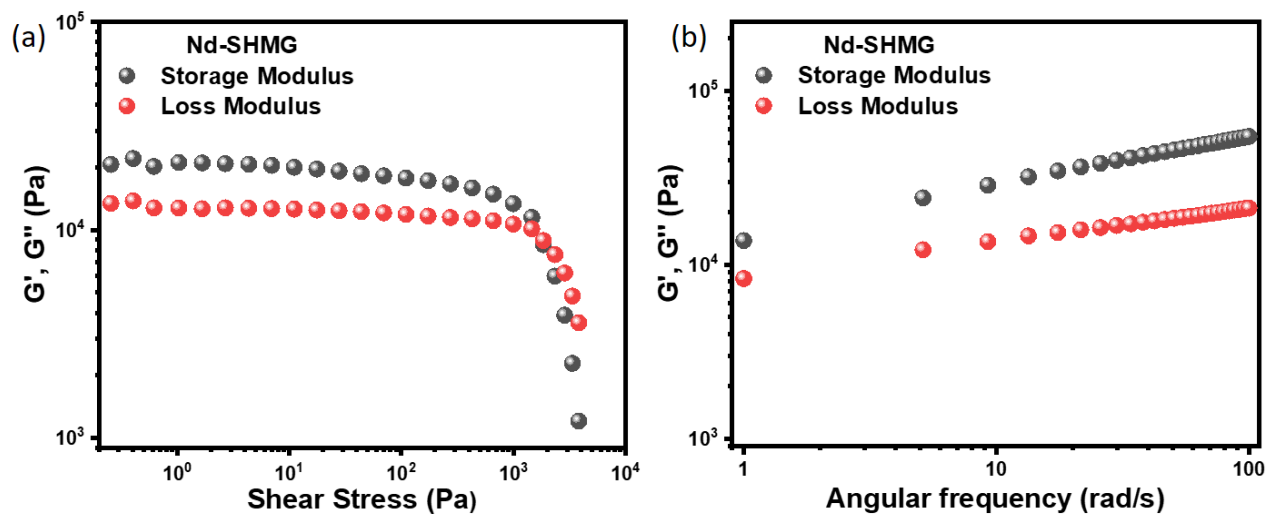


Figure S1. The storage modulus and loss modulus measurement of Nd-SHMG-metallogel with (a) shear stress, and (b) angular frequency.

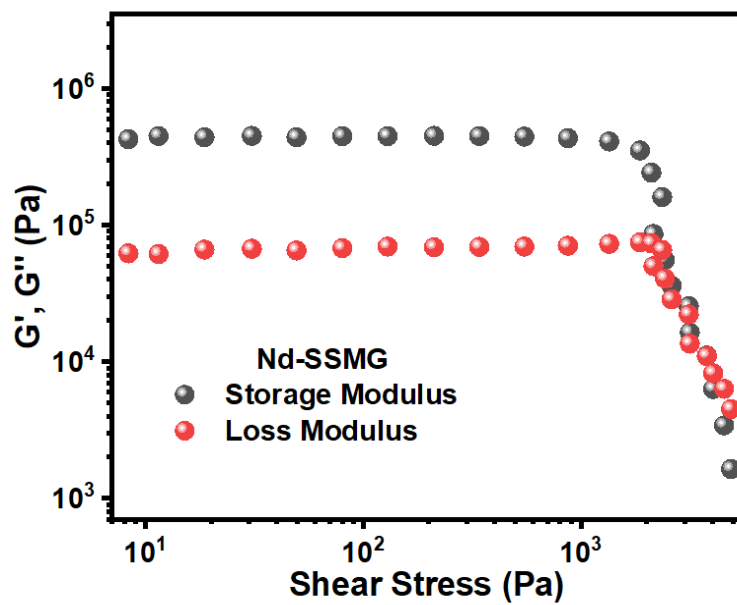


Figure S2. Dynamic shear stress sweep vs. gain modulus (G') and loss modulus (G'') of Nd-SSMG metallogel.

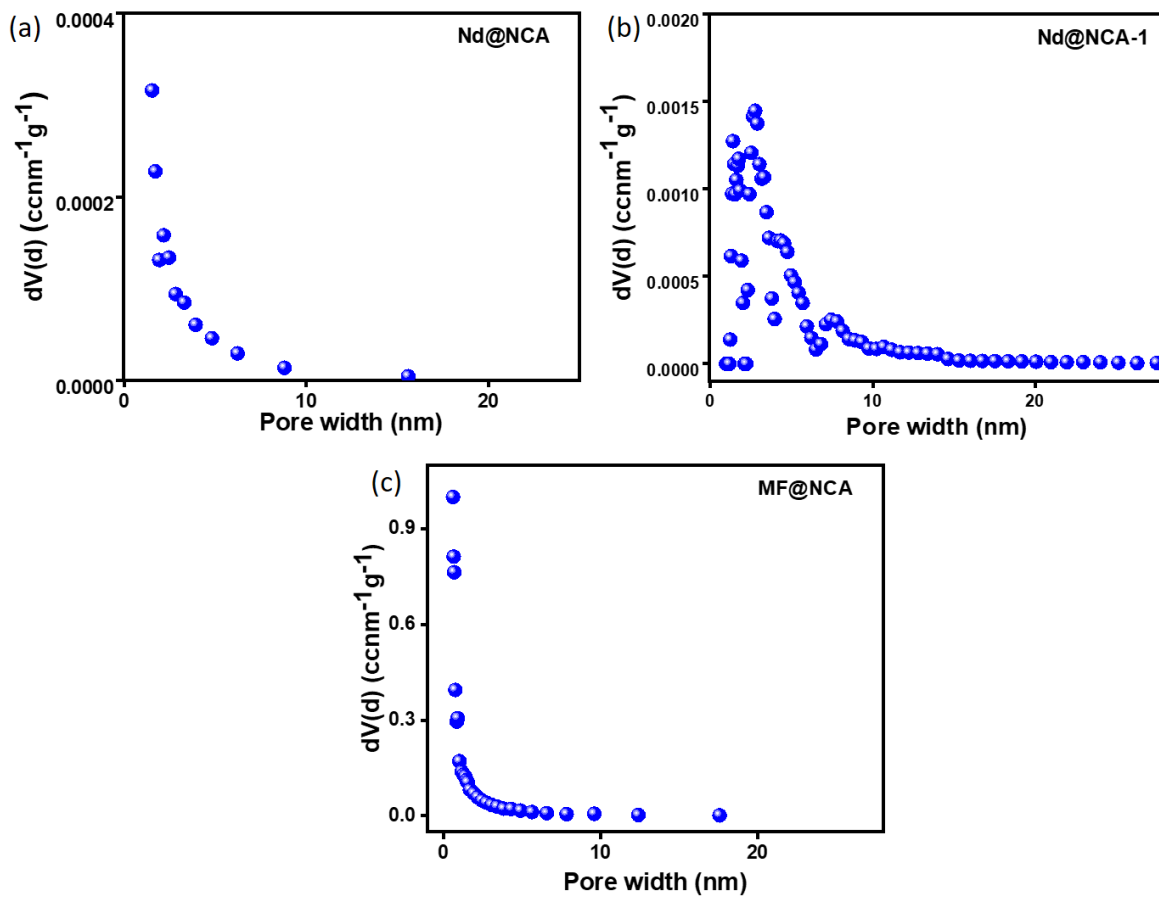


Figure S3. Pore size distribution of Nd@NCA, Nd@NCA-1 and MF@NCA catalysts.

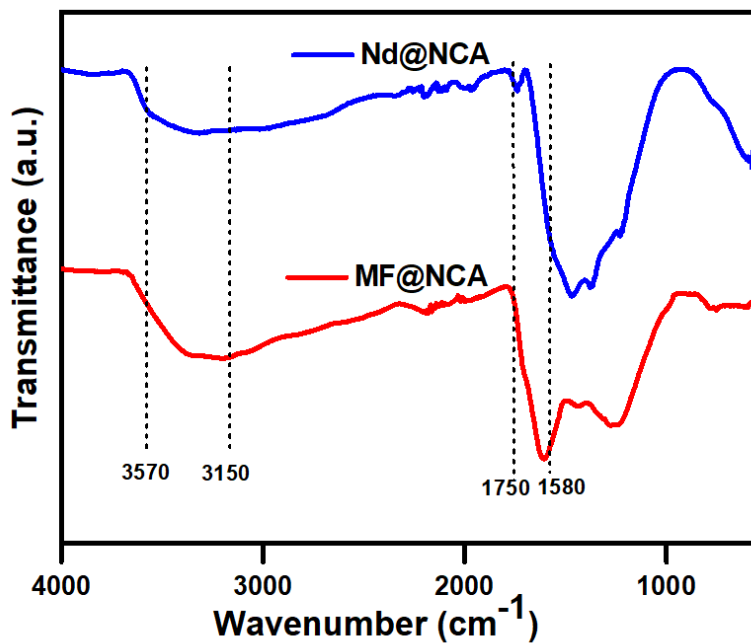


Figure S4. FTIR spectra of Nd@NCA and MF@NCA catalysts.

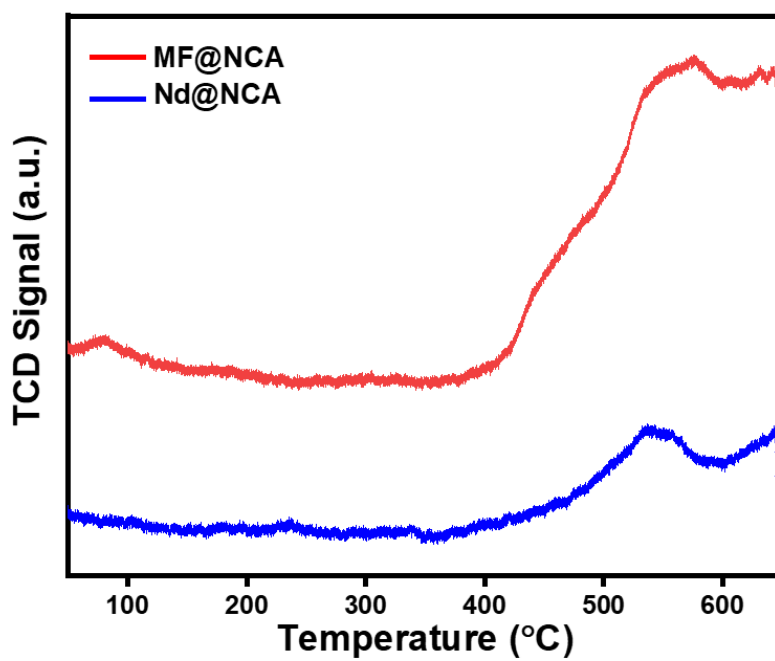


Figure S5. CO₂-TPD analysis of **Nd@NCA** and **MF@NCA** catalysts.

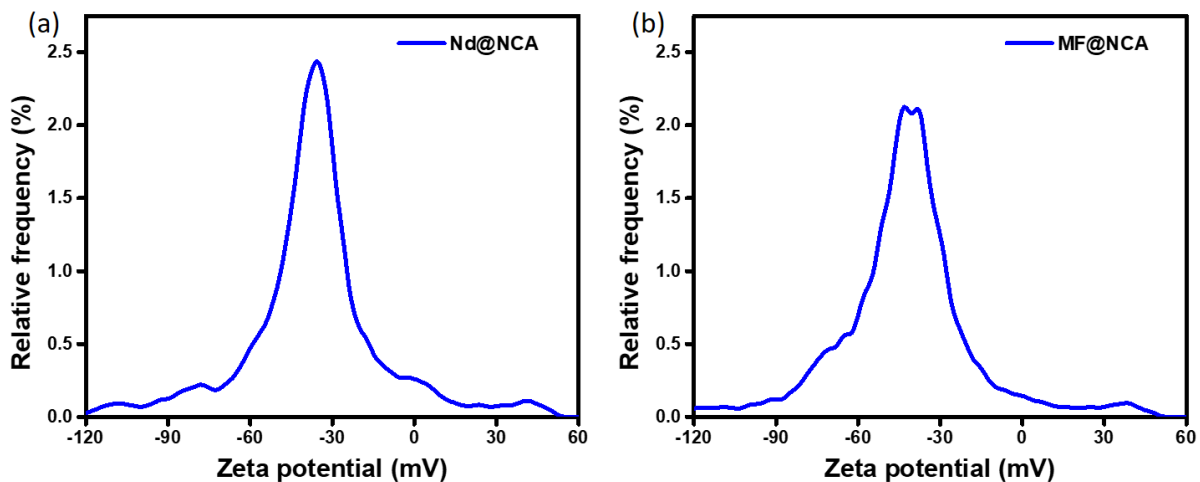


Figure S6. Zeta potential plot of Nd@NCA and MF@NCA catalysts.

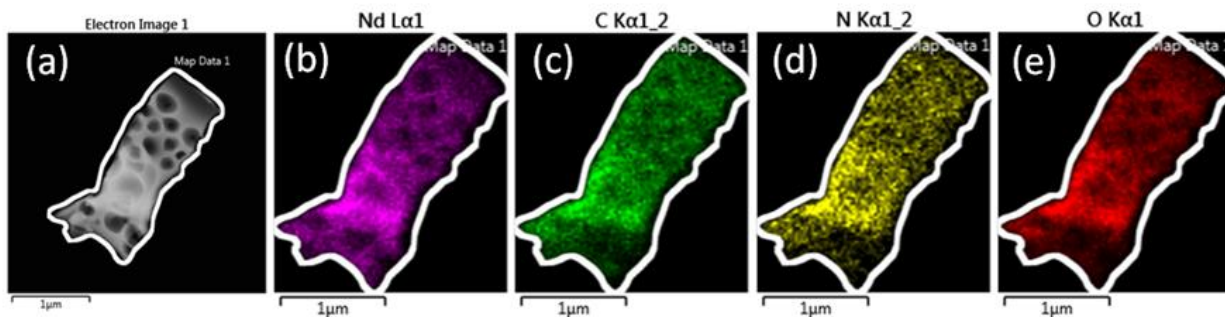


Figure S7. (a-e) Elemental mapping of Nd@NCA catalyst.

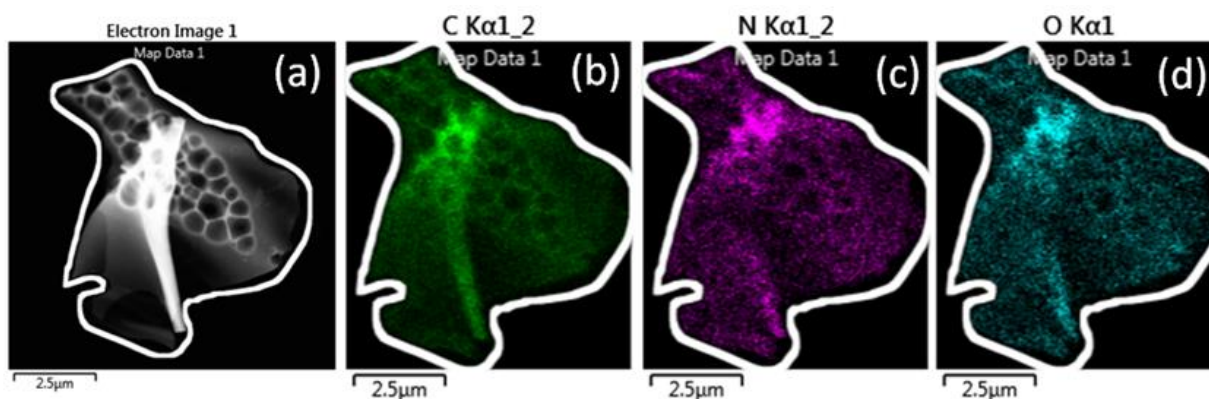


Figure S8. (a-d) Elemental mapping of MF@NCA catalyst.

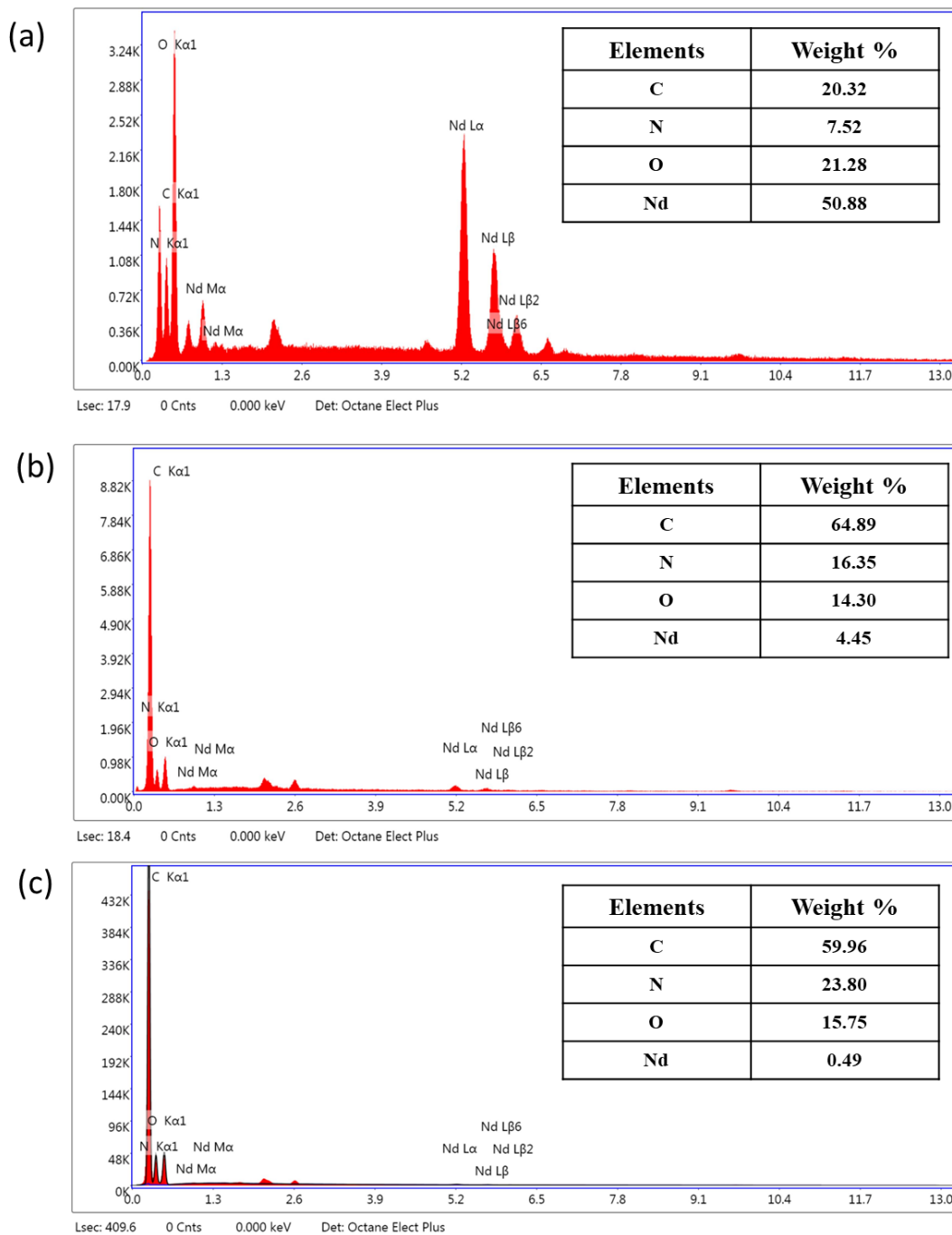


Figure S9. EDX images of Nd@NCA and Nd@NCA-1 and MF@NCA catalysts.

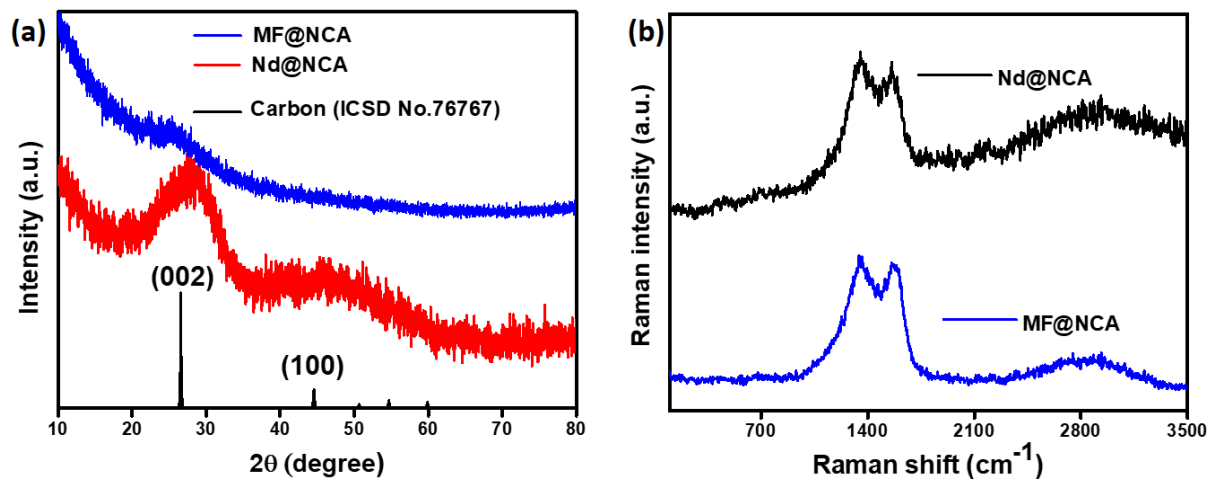


Figure S10. (a) The powder X-ray diffraction pattern of Nd@NCA, MF@NCA catalysts, and Carbon (ICSD database reference: 76767), (b) Raman analysis of Nd@NCA, and MF@NCA catalysts.

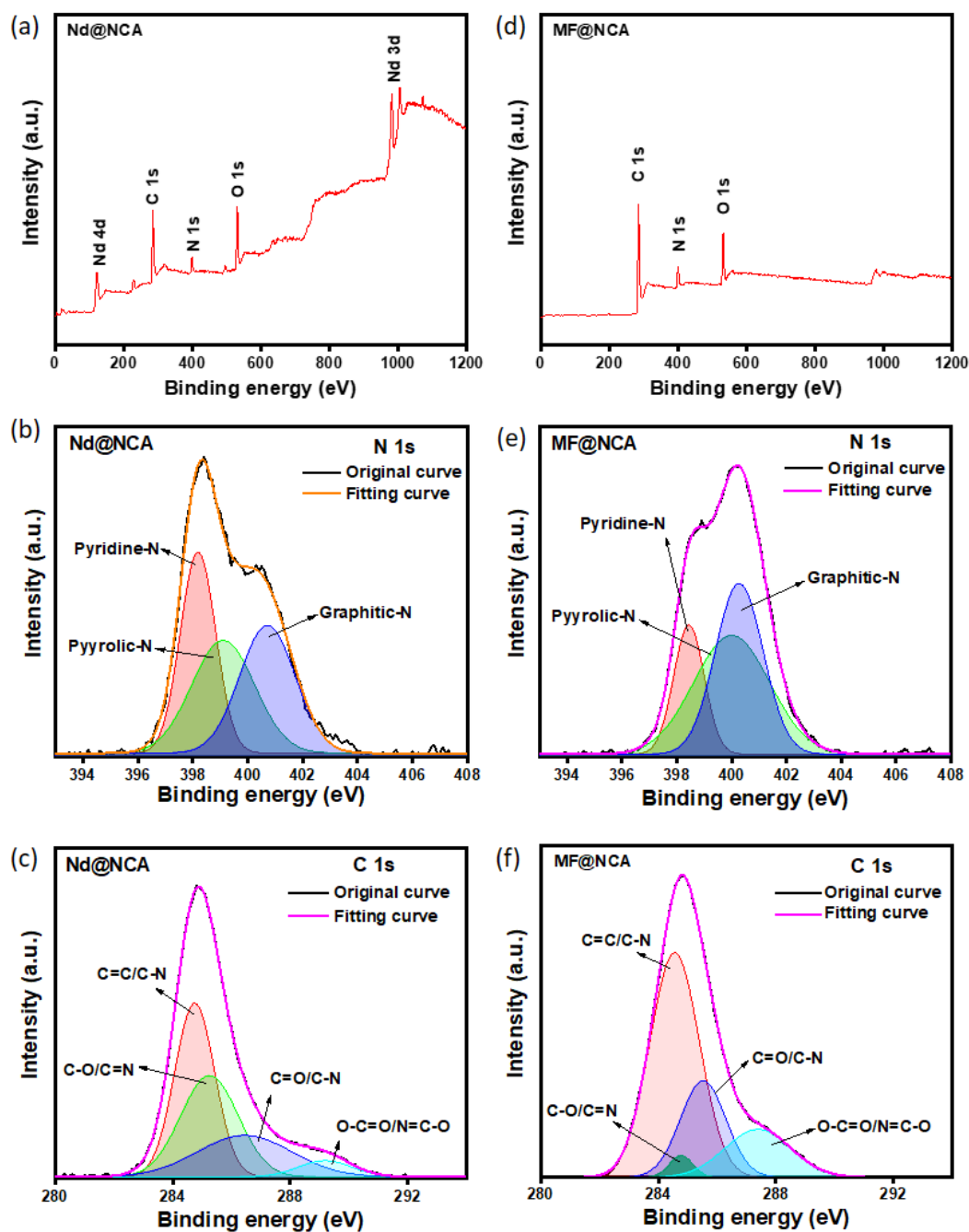


Figure S11. XPS survey of (a) Nd@NCA, the deconvoluted peaks of (b) N 1s, and (c) C 1s for Nd@NCA. XPS survey of (d) MF@NCA, the deconvoluted peaks of (e) N 1s, and (f) C 1s for MF@NCA.

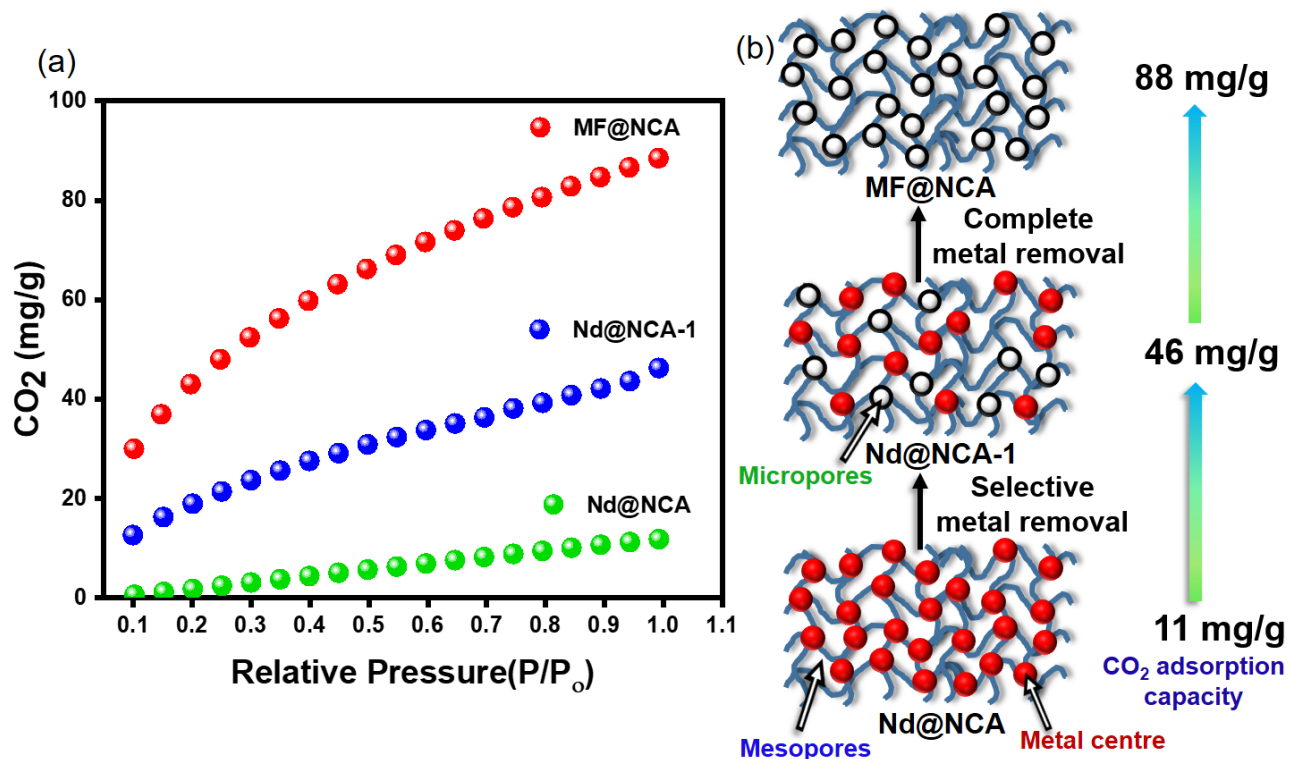


Figure S12. (a) CO₂ adsorption capacity of Nd@NCA, Nd@NCA-1 and MF@NCA catalysts. (b) Schematic illustration for the preparation of porous Nd@NCA-1, and MF@NCA materials through selective removal of metal from the pristine Nd@NCA catalyst.

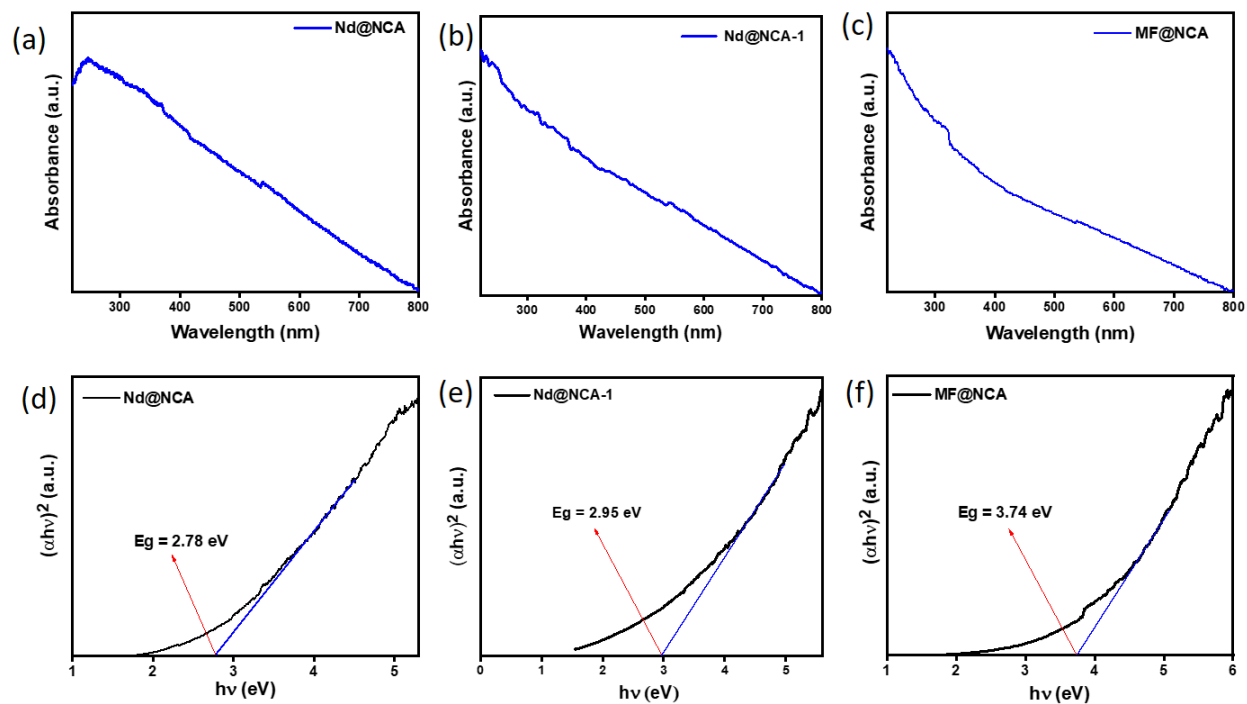


Figure S13. UV-vis absorption spectra of (a) **Nd@NCA**, (b) **Nd@NCA-1**, and (c) **MF@NCA** catalysts, and Tauc's plots of (d) **Nd@NCA**, (e) **Nd@NCA-1**, and (f) **MF@NCA** catalysts.

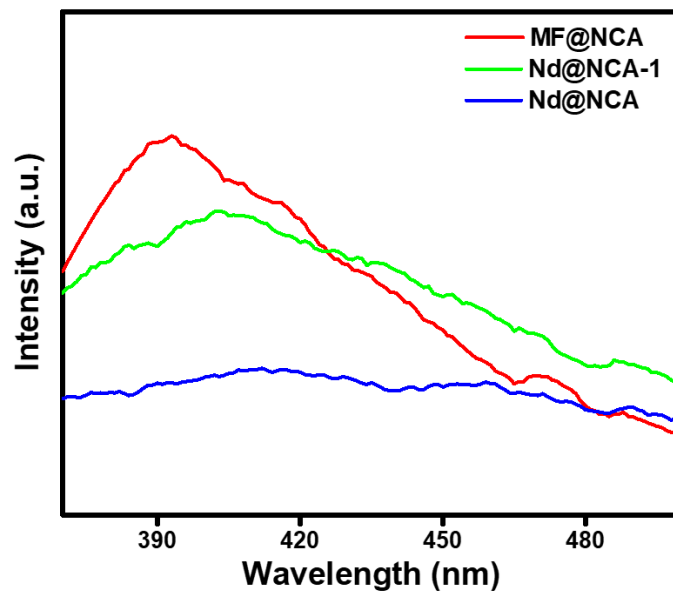


Figure S14. Photoluminescence spectra of Nd@NCA, Nd@NCA-1 and MF@NCA catalysts.

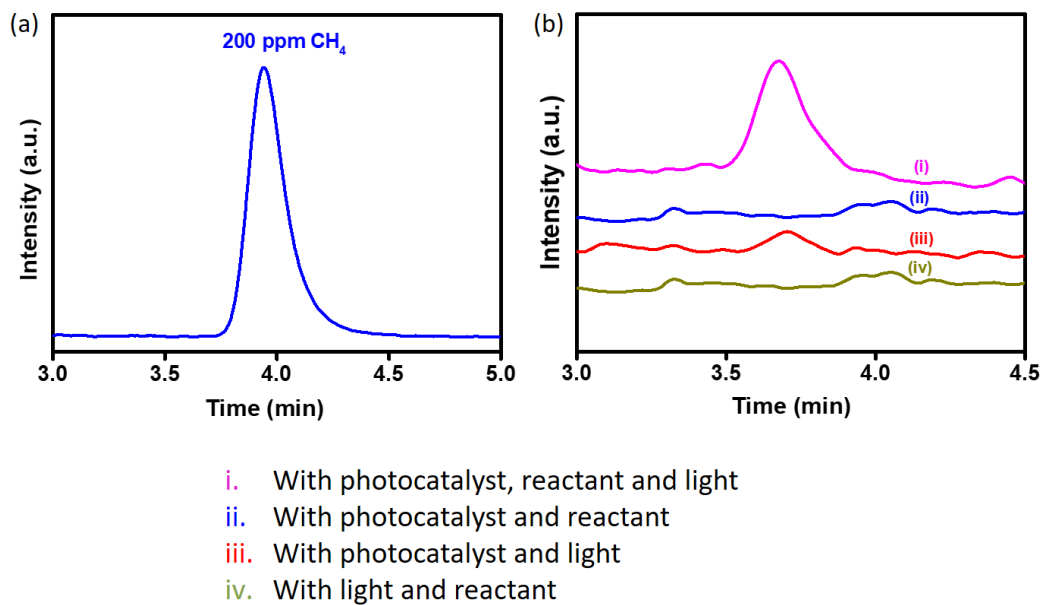


Figure S15. The gas chromatograph for 200 ppm CH₄ present in the standard gas mixture (composition: O₂, H₂, CO and CH₄: 200 ppm each and the rest is argon), (b) Gas chromatograph for various set of controlled/blank measurement.

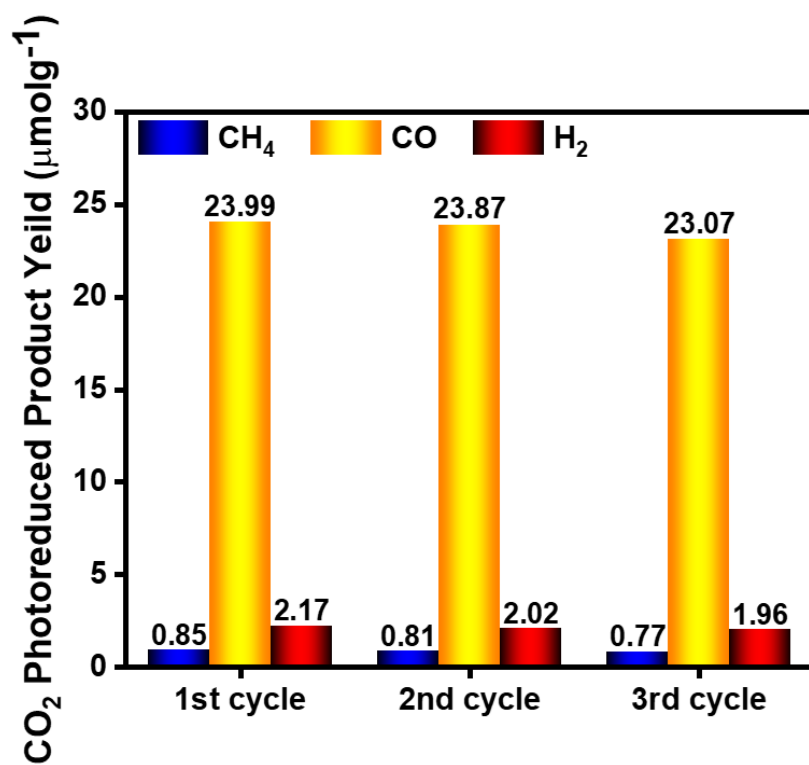


Figure S16. The CO₂ reduced products obtained for Nd@NCA catalyst over three photocatalytic cycles.

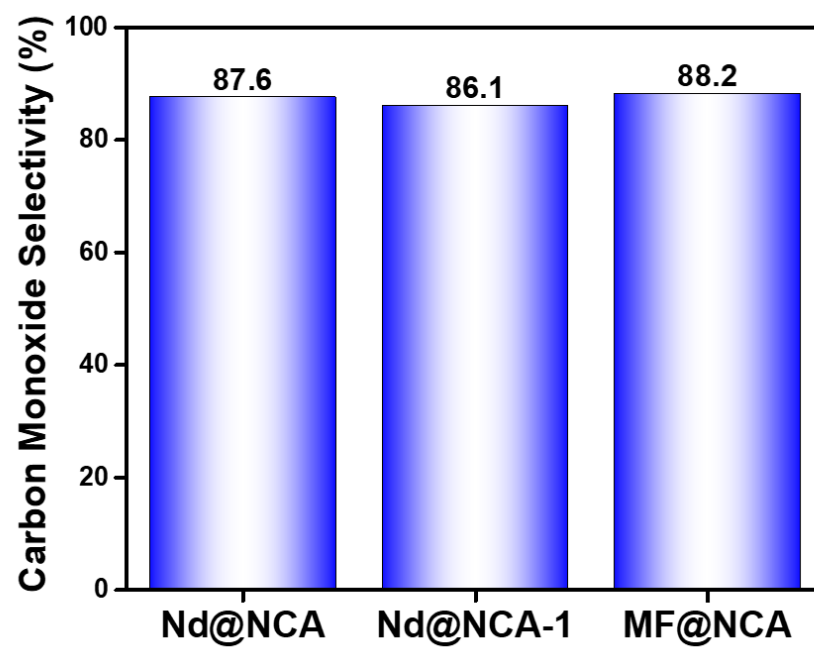


Figure S17. The carbon monoxide selectivity plot of CO over CH₄.

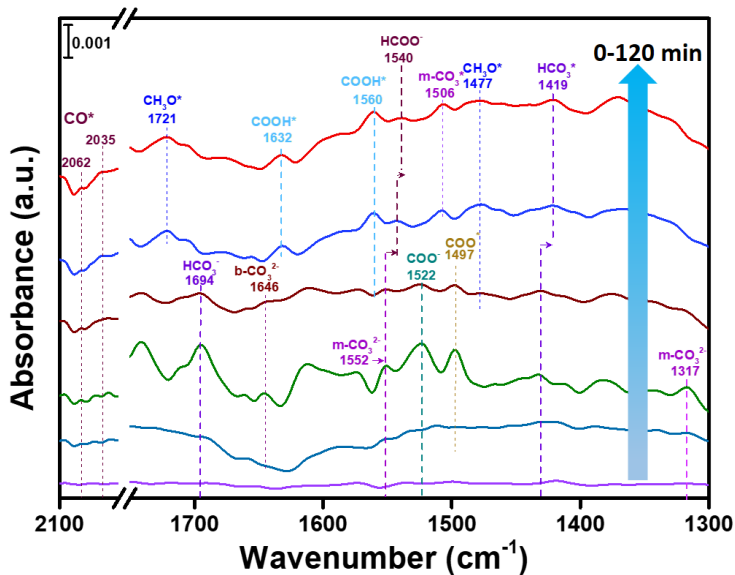


Figure S18. Time-dependent in situ DRIFT analysis for **Nd@NCA** catalyst using moist CO_2 .

Intermediate steps in photocatalytic CO_2 reduction.

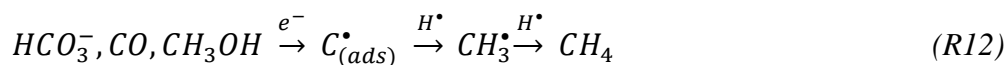
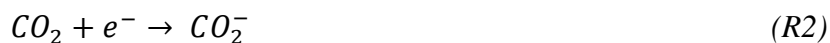


Table S1. Surface area, pore size and pore volume of the as-synthesized catalysts.

Sample name	Surface area (m² g⁻¹)	Pore size (nm)	Pore volume (cc/g)
Nd@NCA	54	3.06	0.058
Nd@NCA-1	231	2.78	0.223
MF@NCA	524	0.62	0.475

Table S2. PL lifetime fitting parameters of Nd@NCA, Nd@NCA-1 and MF@NCA.

	B1(%)	B2(%)	B3(%)	τ1 (ns)	τ2(ns)	τ3(ns)	τ(ns)	χ^2
Nd@NCA	20.21	77.36	2.43	1.84	10.2	0.16	9.819207	1.11
Nd@NCA-1	33.4	60.82	5.78	2.61	9.16	0.5	8.239048	1.05
MF@NCA	21.83	62.14	16.03	1.39	8.42	0.09	8.013997	1.19

Table S3. Comparison table of light driven photocatalytic CO₂ reduction with some of the reported benchmark catalysts.

Material names	Product yield (μmol h ⁻¹ g ⁻¹)	Reaction Conditions	Sacrificial agents	References
(CoPPc)/ (mpg-CN _x)	18.75	CO ₂ /CH ₃ CN/TEOA	TEOA	<i>Angew. Chem. Int. Ed.</i> 2019 , 58, 12180.
MIL-101-Cr	8.3	CO ₂ /H ₂ O/TEOA	TEOA	<i>ACS Appl. Mater. Interfaces</i> 2019 , 11, 27017–27023.
NiCoOP NPs/ [Ru(bpy) ₃]Cl · 6H ₂ O	16.6	CO ₂ /CH ₃ CN/TEOA	TEOA	<i>Angew. Chem. Int. Ed.</i> 2019 , 58, 17236 –17240.
Ni-Complex PS: [Ru(bpy) ₃] Cl ₂	10.2	CO ₂ /DMA, H ₂ O/ BIH	Mg ²⁺	<i>J. Am. Chem. Soc.</i> 2019 , 141, 20309 – 20317.
Ptn/3 DOMSrTiO ₃	4.1	CO ₂ /H ₂ O	--	<i>J. Catal.</i> 2019 377, 309–321.
ZnPorphyrinTTF-COF (TTCOF-Zn)	2.05	CO ₂ /H ₂ O	--	<i>Angew. Chem. Int. Ed.</i> 2019 , 58, 12392 – 12397.
Zn _{0.4} Ca _{0.6} In ₂ S ₄	0.224	CO ₂	--	<i>ACS Appl. Mater. Interfaces</i> 2017 , 9, 27773–27783.
Nd@NCA	~ 2.0	CO ₂ /H ₂ O, at ambient condition	Without any sacrificial agent	This work
Nd@NCA-1	1.46			
MF@NCA	1.4			